Periplasmic domain of the sensor-kinase BvgS reveals a new paradigm for the Venus flytrap mechanism

Julien Herrou[a,b,c,d], Coralie Bompard[e,1], René Wintjens[e,f,1], Elian Dupré[a,b,c,d,1], Eve Willery[a,b,c,d], Vincent Villeret[e], Camille Locht[a,b,c,d], Rudy Antoine[a,b,c,d,2], and Françoise Jacob-Dubuisson[a,b,c,d,2,3]

[a]Institut National de la Santé et de la Recherche Médicale, Center for Infection and Immunity of Lille, F-59019 Lille, France; [b]Institut Pasteur de Lille, F-59019 Lille, France; [c]Université Lille Nord de France, F-59000 Lille, France; [d]Centre National de la Recherche Scientifique, F-59021 Lille, France; [e]Institut de Recherche Interdisciplinaire, Centre National de la Recherche Scientifique, Université de Lille 1–Université de Lille 2, F-59658 Villeneuve d'Ascq, France; and [f]Institut de Pharmacie, Chimie Générale, Université Libre de Bruxelles, 1050 Brussels, Belgium

Two-component sensory transduction systems control important bacterial programs. In *Bordetella pertussis*, expression of the virulence regulon is controlled by the unorthodox BvgAS two-component system. BvgS is the prototype of a family of sensor-kinases that harbor periplasmic domains homologous to bacterial solute-binding proteins. Although BvgAS is active under laboratory conditions, no activating signal has been identified, only negative modulators. Here we show that the second periplasmic domain of BvgS interacts with modulators and adopts a Venus flytrap (VFT) fold. X-ray crystallography reveals that the two lobes of VFT2 delimitate a ligand-binding cavity enclosing fortuitous ligands. Most substitutions of putative ligand-binding residues in the VFT2 cavity keep BvgS active, and alteration of the cavity's electrostatic potential affects responsiveness to modulation. The crystal structure of this VFT2 variant conferring constitutive kinase activity to BvgS shows a closed cavity with another nonspecific ligand. Thus, VFT2 is closed and active without a specific agonist ligand, in contrast to typical VFTs. Modulators are antagonists of VFT2 that interrupt signaling. BvgAS is active for most of the *B. pertussis* infectious cycle, consistent with the proposed mechanism.

bacterial two-component systems | signal transduction | virulence regulation | *Bordetella*

Two-component sensory transduction systems (TCSs) are essential to enable microorganisms to adapt to changes of their environment. TCSs regulate important developmental programs, including virulence, sporulation, competence, or resistance to antimicrobial compounds (1). Ubiquitous in bacteria, they are also found in some higher organisms, such as plants and insects. Typically, they are made of a sensor kinase protein and a cytoplasmic response regulator (RR) (2). The signal is perceived by the sensor, which leads to kinase activation and autophosphorylation of a conserved His residue. The phosphoryl group is then transferred to a conserved Asp residue of the RR. Thus activated, the phosphorylated RR mediates a specific, most frequently transcriptional cellular response (1, 2).

Bordetella pertussis, the whooping cough agent, colonizes the upper respiratory tract of humans (3). Its virulence regulon is controlled by the TCS BvgAS (4). At 37 °C and in commonly used growth media, the sensor kinase BvgS autophosphorylates and transfers its phosphate group via a complex four-step cascade to the final acceptor BvgA. Phosphorylated BvgA activates the transcription of a number of "virulence-activated genes" (*vags*), including those that code for *B. pertussis*'s adhesins and toxins. The Bvg[+] virulent phase of *B. pertussis* is necessary for infection (5). In laboratory conditions, switching to the Bvg[−] avirulent phase is triggered by negative modulators in the culture medium, such as nicotinate or $MgSO_4$ at millimolar concentrations (6). Although BvgAS is central to the pathogenicity of *B. pertussis*, the signals that activate BvgS in vivo or in vitro are unknown. BvgAS is active under laboratory conditions, which may indicate that unlike other TCS sensor kinases, its activation requires no positive sig-

nals, but that it senses only negative signals that switch off its kinase activity.

BvgS is the prototype for a large family of multidomain sensor kinases found in Gram-negative bacteria. The molecular mechanisms of signal perception and transduction by these proteins have remained largely unexplored, in contrast to the extensive studies on classical TCS sensor kinases. BvgS is composed of two periplasmic domains homologous to bacterial periplasmic solute-binding proteins (PBPs) (7), a transmembrane region followed successively by a cytoplasmic PAS (Per/ARNT/SIM), a Histidine-kinase (HK), a receiver and a Histidine phosphotransfer (Hpt) domains (8).

In this work, we investigated the structure and function relationship of the second PBP domain of BvgS. Transport and sensor PBPs adopt a bilobed Venus flytrap (VFT) structure with two mobile jaws delimiting a cavity that binds a specific solute (9). These jaws exist in open and closed conformations, and the binding of a specific ligand in the cavity stabilizes the closed conformation, activating membrane partners for solute import or signaling (10, 11). Several families of eukaryotic receptors, including glutamate-responsive ion channels and metabotropic receptors, harbor VFT domains that function along the same principles as bacterial PBPs (12). BvgS and homologous sensor-kinases represent another class of VFT-containing receptors.

Results

Identification of the BvgS Ligand-Binding Domain. Four recombinant proteins containing periplasmic portions of BvgS were constructed, and their affinities for various small molecules were evaluated (listed in Table 1). The first protein harbors exclusively the two PBP domains in tandem, and the second contains, in addition, a short leucine zipper sequence at the C terminus to mediate dimerization, because TCS sensor-kinases dimerize (13). The other two proteins harbor the PBP domains, VFT1 and VFT2, separately.

Known negative modulators were tested for interaction with these four proteins by using fluorescence spectroscopy (14), but no quenching was detected. Similarly, no potential agonists were identified among the components of the growth medium or the metabolites produced by *B. pertussis* (15). We then used the thermal shift assay (TSA) (16), a technique that has been suc-

MICROBIOLOGY

Table 1. Change of the melting temperature (°C) of the VFT domains in the presence of a ligand

	VFT1	VFT2	VFT2$_{F375E+Q461E}$	VFT2$_{F317A+F375A}$
L-proline	0.55 ± 0.19	−0.03 ± 0.40		
L-cysteine	0.83 ± 0.25	0.55 ± 0.19		
L-serine	0.81 ± 0.27	0.52 ± 0.04		
L-glutamate	0.68 ± 0.23	0.43 ± 0.09		
L-pyroglutamate	0.35 ± 0.13	0.30 ± 0.24		
Oxyded glutathione	0.07 ± 0.48	−0.03 ± 0.41		
Reduced glutathione	0.26 ± 0.25	−0.01 ± 0.18		
Ascorbate	0.70 ± 0.26	1.17 ± 0.43		
Succinate*	0.47 ± 0.18	0.22 ± 0.04		
Fumarate*	0.49 ± 0.20	0.81 ± 0.10		
Formate*	0.26 ± 0.14	−0.01 ± 0.03		
Lactate*	0.56 ± 0.18	0.60 ± 0.15		
Sodium hydroxybutyrate*	0.48 ± 0.05	0.40 ± 0.09		
Acetate*	0.44 ± 0.12	0.44 ± 0.15		
Lithium acetoacetate*	0.07 ± 0.18	−0.29 ± 0.38		
α-ketoglutarate*	0.72 ± 0.06	0.89 ± 0.09		
Pyruvate*	0.88 ± 0.18	1.26 ± 0.27		
MgSO$_4$[†]	−0.90 ± 0.18	0.64 ± 0.21	−0.35 ± 0.42	1.00 ± 0.30
Nicotinate[†]	0.50 ± 0.21	**2.31 ± 0.72**	0.38 ± 0.19	**5.01 ± 0.59**
Isonicotinate[†]	0.79 ± 0.31	**3.35 ± 0.83**	0.53 ± 0.29	**4.91 ± 0.67**
6-hydroxy nicotinate[†]	0.69 ± 0.28	**3.38 ± 0.88**	0.64 ± 0.21	**2.60 ± 0.39**
6-chloro nicotinate[†]	0.06 ± 0.06	1.47 ± 0.46	0.20 ± 0.04	**3.00 ± 0.38**
Pyridine-2.5-dicarboxylate[†]	1.11 ± 0.34	**4.83 ± 1.85**	0.94 ± 0.17	**4.78 ± 0.84**
Quinaldate[†]	−0.36 ± 0.18	**3.80 ± 0.88**	−0.35 ± 0.30	**11.19 ± 1.18**
Benzoate[†]	0.14 ± 0.28	**2.88 ± 1.19**	0.03 ± 0.49	**7.85 ± 1.20**
Sodium salicylate	−0.73 ± 0.15	**3.35 ± 0.72**	−0.19 ± 0.30	**10.61 ± 1.16**
Nicotinamide	−0.44 ± 0.15	0.27 ± 0.25	−0.07 ± 0.02	0.52 ± 0.10
Imidazole	−0.19 ± 0.20	−0.13 ± 0.14	−0.55 ± 0.03	−0.30 ± 0.19
Histidine	0.77 ± 0.10	−0.13 ± 0.15	−0.10 ± 0.20	−0.05 ± 0.32

A thermal shift higher than 2 °C (in bold) is considered to be significant.
*Molecules that accumulate in the culture medium during bacterial growth. All molecules were tested at 30 mM except for 6-chloro nicotinate (16 mM) and pyridine-2.5-dicarboxylate (25 mM).
[†]Negative modulators of virulence (6). In the present work, salicylate was found to modulate virulence at high concentration. The molecules tested by spectrofluorescence are shown in italics.

cessfully applied to PBP–ligand interaction studies (17). The ligands were tested with the single-domain proteins (Table 1). No ligand was found to increase the melting temperature, Tm, of VFT1. In contrast, the Tm of VFT2 was increased by the addition of nicotinic acid or other negative modulators harboring an aromatic cycle at high millimolar concentrations (6) (Table 1). All together, there was a good correlation between the ability to stabilize VFT2 in vitro and the modulating effect in vivo.

X-Ray Structure of the Second BvgS Domain. Given the role of VFT2 in binding BvgS modulators, we determined its X-ray crystal structure to a resolution of 2.04 Å (*SI Appendix*, Table S1). Disordered regions comprise the first 16 N-terminal residues harboring a 6-His tag and the 16 C-terminal residues that are thus not included in the model. Additional electron density in the crystal structure that does not correspond to the protein was attributed to molecules from the crystallization buffer. VFT2 adopts the classic bilobed PBP architecture consisting of two similar α/β domains, lobes I and II (Fig. 1A). The two lobes form a deep cleft and are connected by a hinge region containing a pair of β-strands. Lobe I is composed of residues 292 to 394 and 489 to 526 and includes both the NH$_2$ and COOH termini. Based on the classic VFT paradigm, a putative ligand-binding site is located in the cleft, and a close inspection of the structure indicated distinct electron densities. Two molecules of acetate (Act1 and Act2) and a molecule of glycerol (Gol1) fit the additional density. Act1 is deeply buried and interacts with lobe I by one H bond and a few van der Waals interactions. All other H

bonds are water-mediated (Fig. 1B). Act2 and Gol1 interact essentially with lobe II via a network of water-mediated H-bonds and van der Waals contacts (Fig. 1C).

Thus, VFT2's cavity is filled with water molecules and three fortuitous ligands rather than a single one, arguing against their being bona fide ligands. The interactions between VFT2 and these molecules involve few direct H bonds, but mostly water-mediated H bonds and van der Waals interactions.

Structural Comparisons. The VFT2 structure was compared with those of homologs using the DALI software. Among the first hits were a sensor domain of a HK protein from *Geobacter sulfurreducens* (PDB code 3H7M) (18) and the liganded glutamine-binding protein (GlnBP, 1WDN) of *Escherichia coli*. The structure of GlnBP in open, unliganded form is also available (1GGG). The structures of other bacterial PBPs and eukaryotic VFT domains were included as well.

The value of the opening angle between the lobes was determined for each structure (*SI Appendix*, Table S2). In VFT2, it was 38.8°, very similar to that of its homolog of *G. sulfurreducens* (36.6°). The angles determined for the other proteins vary between 27° and 43.7° for the closed forms and between 52 and 64.9° for the open forms, showing that VFT2 is closed.

The unliganded structure of GlnBP was used to construct open models for the other proteins, enabling us to compare the overall cavity electrostatic potentials as in ref. 19. Remarkably, VFT2 has a strongly positive potential, quite unusual among VFT domains (*SI Appendix*, Fig. S3).
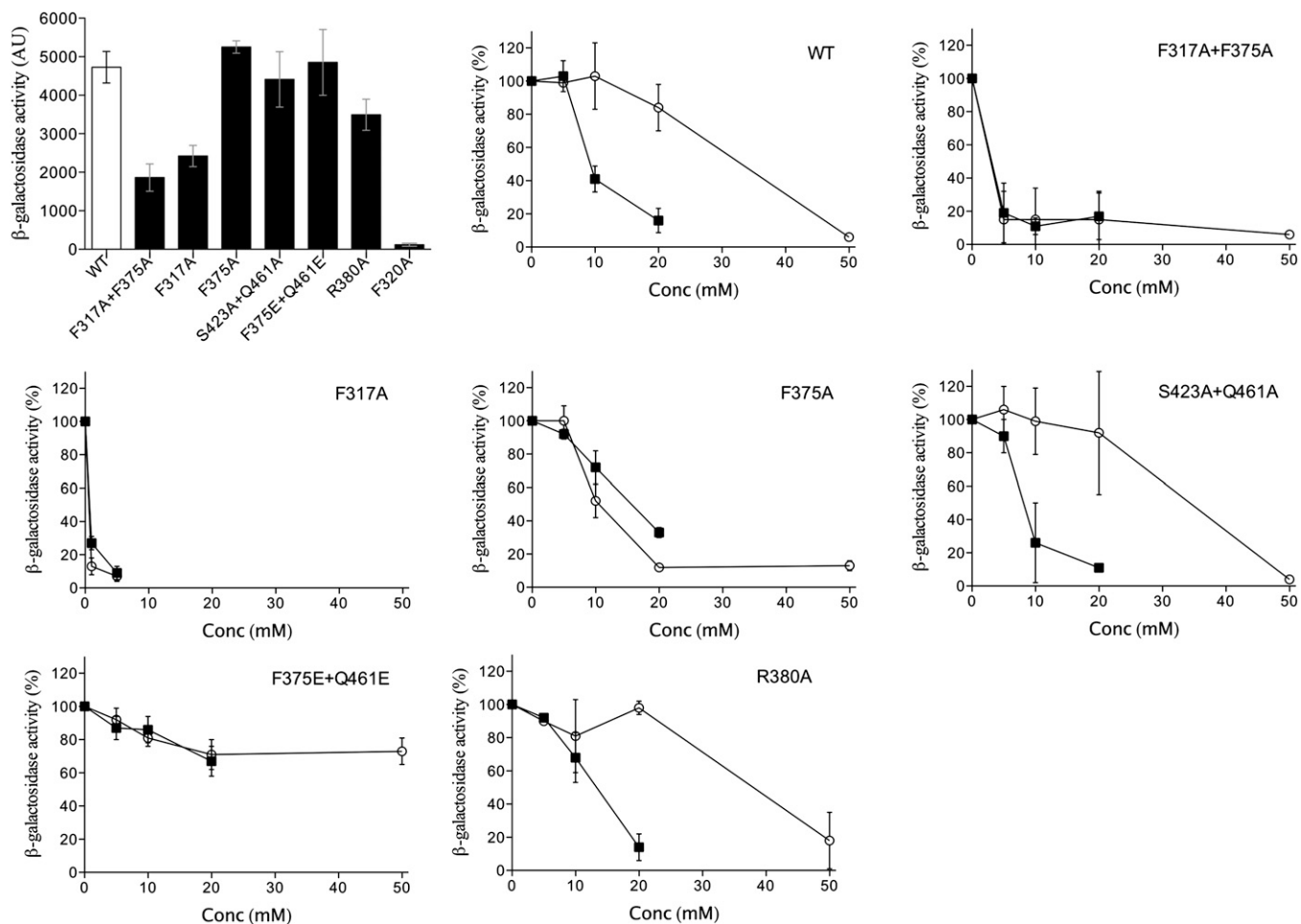
Fig. 1. X-ray structure of VFT2. (*A*) The overall structure of the protein is represented as a ribbon diagram, with the acetate and glycerol molecules shown as red and green sticks, respectively. Lobe 1 is at the left and the two-stranded hinge (S7 and S13) is in the middle. α-Helices and β-strands have been colored cyan and magenta, respectively. VFT2 also harbors two 3_{10} helices, H4 and H5. (*B* and *C*) Major interactions between the molecules present in the VFT2 cavity and the lobes of the protein (*B*, acetates and *C*, glycerol). Lobes I and II are in pale green and orange, respectively, with the hinge strands shown in gray. The H bonds are shown as dotted yellow lines and the H_2O molecules as red spheres. For the sake of clarity, Van der Waals interactions are not represented.

Effect of Altering the Electrostatic Potential of the VFT2 Cavity. To probe the function of the VFT2 cavity, we altered its electrostatic potential by mutagenesis (*SI Appendix*, Fig. S3). Mutations were introduced into *B. pertussis bvgS*. A *lacZ* reporter under the

control of the Bvg-regulated *ptx* promoter was used to assess the function of the system in vivo after growing the recombinant bacteria in the presence or absence of the negative modulators $MgSO_4$ or nicotinic acid (20). BvgS-VFT2$_{F375E+Q461E}$ was fully active but insensitive to modulation (Fig. 2).

Recombinant VFT2$_{F375E+Q461E}$ was analyzed by TSA. It was slightly more stable than VFT2, but its Tm was not increased by aromatic modulators (Table 1). The X-ray structure of VFT2$_{F375E+Q461E}$ was also determined (*SI Appendix*, Table S1). Although the protein crystallized in different conditions than its counterpart, the two structures are very similar, with a rmsd value of 1.1 Å for Cα atoms superposition (*SI Appendix*, Fig. S4). The cavity of VFT2$_{F375E+Q461E}$ is also closed (*SI Appendix*, Table S2) but instead of acetate and glycerol, ethylene glycol—probably from the crystallization medium—was found inside. The increased stability and closed conformation of VFT2$_{F375E+Q461E}$ could be explained by additional, direct interactions between residues of the two lobes probably caused by the introduction of the two Glu side chains (*SI Appendix*, Fig. S5).

Effect of Substitutions in the VFT2 Cavity. The VFT2 cavity is totally conserved among a large number of *Bordetella* isolates (20), arguing that it is highly adapted to function. To identify functionally important cavity motifs, we performed structure-based comparisons with its closest homologs (*SI Appendix*, Fig. S6). Several cavity residues that bind the fortuitous ligands correspond to ligand-binding residues in homologs (Fig. 1 and *SI Appendix*, Fig. S6). We thus investigated their role for BvgS activity.

In amino acid-binding PBPs related to VFT2, a salt bridge between a conserved Arg and the α-carboxyl group of the ligand, which significantly contributes to PBP-ligand affinity (21). Although an Arg residue is present at the same position in VFT2, its substitution did not affect the in vivo activity of BvgS-VFT2$_{R380A}$ or its response to modulation (Fig. 2).

Phe$_{317}$ and Phe$_{375}$ of lobe I participate in the cavity binding network (Fig. 1). BvgS-VFT2$_{F317A+F375A}$ had an intermediate level of activity and was extremely sensitive to negative modulation (Fig. 2). By TSA, the stability of VFT2$_{F317A+F375A}$ was decreased compared with that of VFT2, but its Tm was strongly increased by aromatic modulators (Table 1). BvgS-VFT2$_{F317A}$ had a phenotype very similar to that of VFT2$_{F317A+F375A}$, but the phenotype of VFT2$_{F375A}$ was closer to that of wt BvgS (Fig. 2). Thus, it is essentially the F$_{317}$ side chain that contributes to maintaining VFT2 in an active conformation and restrains modulator binding. Attempts to crystallize this variant with a modulator were unsuccessful.

F$_{320}$ is in a β-turn in the vicinity of F$_{317}$ and partially accessible in the cavity; its replacement by Ala totally abolished BvgS activity (Fig. 2). By TSA, VFT2$_{F320A}$ was significantly destabilized compared with VFT2, with a Tm decrease of ≈ 9 °C, and modulator binding restabilized it by 2 to 4 °C. Finally, a double S$_{423}$A+Q$_{461}$A substitution introduced in two putative binding motifs of lobe II did not affect the activity of BvgS or its response to modulation (Fig. 2).

Discussion

A large group of sensor proteins of TCS contain periplasmic domains homologous to PBPs, whose mode of action has remained undeciphered. With transport PBPs, binding of a ligand in the cavity favors the closed conformation (10, 11, 22), which allows the protein to interact specifically with the membrane transporter for solute import (23). A related "PBP model" also applies to eukaryote receptors harboring VFT domains, notably ionotropic Glu receptors, for which the binding of an agonist closes the VFT cavity and triggers a response in the form of ion channel opening (12, 24). In contrast, although the second BvgS domain adopts a typical VFT fold, VFT2 represents a previously unexplored paradigm. Our data strongly support the

Fig. 2. β-gal activities of recombinant strains harboring BvgS variants with substitutions in the VFT2 cavity. A *lacZ* reporter placed under the control of the Bvg-regulated *ptx* promoter was used to assess Bvg activity. The first panel shows the activities of the various strains grown in SS medium in the absence of modulation calculated as in ref. 31. The effects of the negative modulators $MgSO_4$ (○) and nicotinic acid (■) on β-gal activity are shown in the remaining panels, where 100% represents the activity of bacteria grown without modulators.

model that VFT2 is in a closed conformation and active by default and binds only antagonists.

VFT2 crystallized in a closed conformation, with several small molecules that have few direct interactions with the cavity walls and essentially with only one lobe or the other, arguing that they are fortuitous ligands. The homologous VFT domain of the *G. sulfurreducens* sensor kinase was also found closed with only water molecules in its cavity. It is most likely not a coincidence that neither it nor VFT2 have trapped authentic ligands while crystallizing in closed conformations. Although BvgS's VFT2 is a close homolog of amino acid binding PBPs, mutagenesis of its cavity showed that it has functionally diverged from the latter group. In contrast with those PBPs, few replacements of residues involved in the interaction network of the VFT2 cavity affected BvgS activity, arguing that it has lost the capacity to bind high-affinity agonist ligands. Furthermore, the constitutively active BvgS$_{F375E+Q461E}$ variant strongly indicates that the closed conformation is the active form of VFT2 and that no bona fide agonist in the VFT2 cavity is needed for BvgS activity. This finding is in contrast with the VFT sensors of eukaryotic receptors, which are off by default and respond specifically to the presence of agonists to activate the system.

The importance of the dynamic properties of signaling proteins is now recognized as crucial to their functions (25). Thus, the active state of VFT2 allows the action of modulating an-

tagonists, unlike the constitutively active variant with a lesser positive electrostatic cavity potential, which no longer binds nicotinate in vitro or in vivo. Therefore, we propose that in BvgS VFT2 has evolved both to adopt an active conformation without a specific ligand and to respond to negative modulation. In vitro, the soluble cytoplasmic portion of BvgS has kinase activity by itself (26). In contrast, in vivo the complete loss of activity caused by the single $F_{320}A$ substitution shows that in full-length BvgS the kinase needs an activating signal from the upstream periplasmic domain. Thus, the default state of the periplasmic domain of BvgS provides an activating signal for the cytoplasmic kinase, which is transmitted mechanically through the membrane. For VFT2, this active state corresponds to a closed conformation. The unusually positive electrostatic potential of the VFT2 cavity is most likely also an important piece of the molecular mechanism of the periplasmic domain of BvgS. Thus, we propose that the positive charges of the two lobes are partially screened by nonspecific ligands found in the milieu, stabilizing the closed conformation. This finding is consistent with the observation that various organic and inorganic ions influence the activity of BvgS in the bacterium (27). The electrostatic potential of VFT2 also allows the action of antagonists, consistent with the fact that a major feature of organic negative modulators is their carboxylate group (6), whose charge is complementary to that of the VFT2 cavity.

In laboratory conditions, nicotinate is an antagonist, albeit a poor one, which is active at millimolar concentrations. We propose that nicotinate binds to the VFT2 cavity most likely by outcompeting nonspecific ligands and modifies the conformation of the protein, turning it into an inactive state. This conformational change interrupts the transmission of the activating signal to the kinase. We have identified two Phe residues whose replacement affects the activity of BvgS. F_{317} and F_{320} are located close to each other in a β-turn that precedes a long surface-oriented loop. Both VFT2$_{F317A}$ and VFT2$_{F320A}$ are less stable than VFT2, thus linking BvgS function to the structure of this region. Interestingly, Bvg-VFT2$_{F317A}$ is also very sensitive to nicotinate, which suggests that nicotinate binds in this area of the VFT2 cavity. The possibility that the conformation of this turn-and-loop region participates in signaling by BvgS will be investigated in future work.

Thus, BvgS has evolved to be active unless specific negative signals are present in the environment, which may be the most appropriate type of regulation for the lifestyle of *B. pertussis*. Although the cost of virulence factor production by default appears to be high, this strategy may be rational for a pathogen that is directly transmitted from host to host and absolutely requires the Bvg$^+$ phase for colonization and development of the infection. Nevertheless, BvgS has maintained its capacity to respond to negative signals rather than being constitutively active, although constitutive variants appear readily in laboratory conditions (28). *B. pertussis* is able to survive and replicate in macrophages (29), and its persistence in intracellular niches might contribute to the prolonged disease that it causes. The downregulation of Bvg-regulated adenylate cyclase upon entry in macrophages has been reported (30). Thus, specific modulators present in certain intracellular compartment where *B. pertussis* can reside may be natural VFT2 antagonists that turn off BvgS.

We have deciphered the molecular mechanism of VFT2 and established a unique paradigm in VFT-containing proteins. BvgS also contains the VFT1 domain, whose contribution to the activity of BvgS remains to be determined. A domain organization similar to that of BvgS is found in a large number of nonorthodox TCS sensor-kinases, with two extracytoplasmic VFT domains in tandem (http://mistdb.com/). This highly conserved architecture further argues that the two domains function together in a precise manner that eventually determines the level of activation of the protein. Deciphering their dialogue will be helpful to understand the molecular mechanisms of these complex sensor kinases.

Materials and Methods

Protein Production and Purification. VFT1 and VFT2 encompass S_{30} to S_{287} and L_{288} to I_{542}, respectively. All oligonucleotides and construction details are given in *SI Appendix*, Table S7. Recombinant proteins were produced using standard techniques and purified by metal-chelate affinity chromatography.

Biochemical Techniques. TSA was performed in 96-well plate with 30 μM protein, 4× NanoOrange (Invitrogen) and 30 mM of each chemical compound to be tested, adjusted to pH 7.4. The plates were heated to 85 °C with a ramp rate of 0.07 °C/s and read by a thermocycler (LightCycler 480 II; Roche) using excitation and emission wavelengths of 465 nm and 510 nm, respectively. The Tm values were determined using the LightCycler480 Software. The experiments were performed two or three times in triplicate. In each experiment the variation of Tm in the presence of each ligand was calculated, and the SD between experiments was determined.

Crystal Structure Determination. All experimental details are given as *SI Text*. The Rfree factors for VFT2 and VFT2$_{F375E+Q461E}$ were 21.86% and 24.57%, respectively.

Characterization of the VFT2 Substitutions. Mutations were introduced by overlapping PCR. The mutated fragments were introduced in a suicide plasmid used for allelic exchange (20). The *S1-lacZ* fusion was introduced into the recombinant strains using pFUS2 (31), and β-gal activities were measured as in ref. 20. At least three independent measurements were performed. The presence of BvgS-VFT2$_{F320A}$ was verified by immunoblotting.

1. Bekker M, Teixeira de Mattos MJ, Hellingwerf KJ (2006) The role of two-component regulation systems in the physiology of the bacterial cell. *Sci Prog* 89:213–242.
2. Stock AM, Robinson VL, Goudreau PN (2000) Two-component signal transduction. *Annu Rev Biochem* 69:183–215.
3. Hewlett EL (1997) *Pertussis*: Current concepts of pathogenesis and prevention. *Pediatr Infect Dis J* 16(4, Suppl)S78–S84.
4. Stibitz S (2007) The Bvg regulon. *Bordetella Molecular Biology*, ed Locht C (Horizon Bioscience, Norfolk, United Kingdom), pp 47–68.
5. Cotter PA, Jones AM (2003) Phosphorelay control of virulence gene expression in *Bordetella. Trends Microbiol* 11:367–373.
6. Melton AR, Weiss AA (1993) Characterization of environmental regulators of *Bordetella pertussis. Infect Immun* 61:807–815.
7. Martínez de Tejada GM, Miller JF, Cotter PA (1996) Comparative analysis of the virulence control systems of *Bordetella pertussis* and *Bordetella bronchiseptica. Mol Microbiol* 22:895–908.
8. Uhl MA, Miller JF (1994) Autophosphorylation and phosphotransfer in the *Bordetella pertussis* BvgAS signal transduction cascade. *Proc Natl Acad Sci USA* 91:1163–1167.
9. Quiocho FA, Ledvina PS (1996) Atomic structure and specificity of bacterial periplasmic receptors for active transport and chemotaxis: Variation of common themes. *Mol Microbiol* 20:17–25.
10. Oh BH, et al. (1993) Three-dimensional structures of the periplasmic lysine/arginine/ornithine-binding protein with and without a ligand. *J Biol Chem* 268:11348–11355.
11. Trakhanov S, et al. (2005) Ligand-free and -bound structures of the binding protein (LivJ) of the *Escherichia coli* ABC leucine/isoleucine/valine transport system: Trajectory and dynamics of the interdomain rotation and ligand specificity. *Biochemistry* 44:6597–6608.
12. Furukawa H, Singh SK, Mancusso R, Gouaux E (2005) Subunit arrangement and function in NMDA receptors. *Nature* 438:185–192.
13. Casino P, Rubio V, Marina A (2009) Structural insight into partner specificity and phosphoryl transfer in two-component signal transduction. *Cell* 139:325–336.
14. Miller DM, 3rd, Olson JS, Pflugrath JW, Quiocho FA (1983) Rates of ligand binding to periplasmic proteins involved in bacterial transport and chemotaxis. *J Biol Chem* 258:13665–13672.
15. Thalen M, et al. (1999) Rational medium design for *Bordetella pertussis*: Basic metabolism. *J Biotechnol* 75:147–159.
16. Pantoliano MW, et al. (2001) High-density miniaturized thermal shift assays as a general strategy for drug discovery. *J Biomol Screen* 6:429–440.
17. Giuliani SE, Frank AM, Collart FR (2008) Functional assignment of solute-binding proteins of ABC transporters using a fluorescence-based thermal shift assay. *Biochemistry* 47:13974–13984.
18. Cheung J, Le-Khac M, Hendrickson WA (2009) Crystal structure of a histidine kinase sensor domain with similarity to periplasmic binding proteins. *Proteins* 77:235–241.
19. Ledvina PS, Yao N, Choudhary A, Quiocho FA (1996) Negative electrostatic surface potential of protein sites specific for anionic ligands. *Proc Natl Acad Sci USA* 93:6786–6791.
20. Herrou J, et al. (2009) Molecular evolution of the two-component system BvgAS involved in virulence regulation in *Bordetella. PLoS ONE* 4:e6996.
21. Oh BH, et al. (1994) The bacterial periplasmic histidine-binding protein. Structure/function analysis of the ligand-binding site and comparison with related proteins. *J Biol Chem* 269:4135–4143.
22. Björkman AJ, Mowbray SL (1998) Multiple open forms of ribose-binding protein trace the path of its conformational change. *J Mol Biol* 279:651–664.
23. Liu CE, Liu PQ, Wolf A, Lin E, Ames GF (1999) Both lobes of the soluble receptor of the periplasmic histidine permease, an ABC transporter (traffic ATPase), interact with the membrane-bound complex. Effect of different ligands and consequences for the mechanism of action. *J Biol Chem* 274:739–747.
24. Mayer ML, Armstrong N (2004) Structure and function of glutamate receptor ion channels. *Annu Rev Physiol* 66:161–181.
25. Smock RG, Gierasch LM (2009) Sending signals dynamically. *Science* 324:198–203.
26. Perraud AL, Kimmel B, Weiss V, Gross R (1998) Specificity of the BvgAS and EvgAS phosphorelay is mediated by the C-terminal HPt domains of the sensor proteins. *Mol Microbiol* 27:875–887.
27. Lacey BW (1960) Antigenic modulation of *Bordetella pertussis. J Hyg (Lond)* 58:57–93.
28. Manetti R, Aricò B, Rappuoli R, Scarlato V (1994) Mutations in the linker region of BvgS abolish response to environmental signals for the regulation of the virulence factors in *Bordetella pertussis. Gene* 150:123–127.
29. Lamberti YA, Hayes JA, Perez Vidakovics ML, Harvill ET, Rodriguez ME (2010) Intracellular trafficking of *Bordetella pertussis* in human macrophages. *Infect Immun* 78:907–913.
30. Masure HR (1992) Modulation of adenylate cyclase toxin production as *Bordetella pertussis* enters human macrophages. *Proc Natl Acad Sci USA* 89:6521–6525.
31. Antoine R, et al. (2000) New virulence-activated and virulence-repressed genes identified by systematic gene inactivation and generation of transcriptional fusions in *Bordetella pertussis. J Bacteriol* 182:5902–5905.

MICROBIOLOGY